

Sensitivity to Contact Interactions and Extra Dimensions in Di-lepton and Di-photon Channels at Future Colliders

Contribution to LHC / LC Study Group Working Document¹

DIMITRI BOURILKOV
bourilkov@mailaps.org

*University of Florida
Gainesville, FL, USA*

Abstract

Virtual effects from a generic description of physics beyond the Standard Model in terms of contact interactions, or from large extra dimensions will modify the observed cross sections for easy to detect final states like lepton or photon pairs, and can be used to probe scales much higher than the center-of-mass energy of the partons initiating the interactions. In this note the sensitivity reach of the Large Hadron Collider to contact interactions in the Drell-Yan channels and of a Future Linear Collider to contact interactions and extra dimensions in e^+e^- , $\mu^+\mu^-$ and $\gamma\gamma$ final states are studied. Experimental aspects of the measurements, systematic error effects and the evolution of the search reach with accumulated luminosity are considered.

Work presented at the LHC/LC Study Group (CERN 5 July 2002, 14 February and 9 May 2003)

1 Introduction

The Large Hadron Collider (LHC) and a Future Linear Collider (FLC) open complementary possibilities at the high energy frontier. The latter offers the benefits of a well defined initial state while the former can be viewed as a wide band parton beam, capable of probing deep into the TeV region. Many new effects, if discovered at LHC, can be studied in greater detail at a FLC.

The most desirable case is the direct observation of unknown physics phenomena, e.g. a peak in a mass spectrum. Even if we are not so lucky, virtual effects from a generic

¹For further informations, see <http://www.ippp.dur.ac.uk/~georg/lhclc/> . For questions and comments, please contact Georg.Weiglein@durham.ac.uk .

description of physics beyond the Standard Model (SM) in terms of contact interactions, or from large extra dimensions will modify the observed cross sections for easy to detect final states like lepton or photon pairs, and can be used to probe scales much higher than the center-of-mass energy \sqrt{s} of the partons initiating the interactions.

There have been many studies of the sensitivity reach of LHC and a FLC to contact interactions or extra dimensions. Here we will concentrate on some experimental aspects of the measurements, the effects of systematic errors and the evolution of the search reach with accumulated luminosity.

2 Contact Interactions

Contact interactions offer a general framework for describing a new interaction with typical energy scale $\mathbb{L} \gg \sqrt{s}$. The presence of operators with canonical dimension $N > 4$ in the Lagrangian gives rise to effects $\sim 1/M^{N-4}$. Such interactions can occur for instance, if the SM particles are composite, or when new heavy particles are exchanged.

Table 1: Contact interaction models.

Model	LL	RR	LR	RL	VV	AA	LL+RR	LR+RL
	Non-parity conserving				Parity conserving			
η_{LL}	± 1	0	0	0	± 1	± 1	± 1	0
η_{RR}	0	± 1	0	0	± 1	± 1	± 1	0
η_{LR}	0	0	± 1	0	± 1	∓ 1	0	± 1
η_{RL}	0	0	0	± 1	± 1	∓ 1	0	± 1

In the following we will consider fermion- or photon-pair production. In the fermion case, the lowest order flavor-diagonal and helicity-conserving operators have dimension six [1]. For photons the lowest order operators have dimension eight, leading to suppression of the interference terms as the inverse fourth power of the relevant energy scale.

The differential cross section takes the form

$$\frac{d\sigma}{d\Omega} = SM(s, t) + \varepsilon \cdot C_{Int}(s, t) + \varepsilon^2 \cdot C_{NewPh}(s, t) \quad (1)$$

where the first term is the Standard Model contribution, the second comes from interference between the SM and the contact interaction, and the third is the pure contact interaction effect. The Mandelstam variables are denoted as s , t and u .

Usually the coupling is fixed, and the structure of the interaction is parametrized by coefficients for the helicity amplitudes:

$$\begin{array}{ll} \mathbf{g} & \text{coupling (by convention } \frac{g^2}{4\pi} = 1) \\ |\eta_{ij}| \leq 1 & \text{helicity amplitudes } (i, j = L, R) \\ \varepsilon & \frac{g^2 \text{ sign}(\eta)}{4\pi \mathbb{L}^2} \text{ for } f\bar{f}; \sim \frac{1}{\mathbb{L}^4} \text{ for } \gamma\gamma \end{array}$$

Some often investigated models are summarized in Table 1. The models in the second half of the table are parity conserving, and hence not constrained by the very precise

measurements of atomic parity violation at low energies. The results presented in this contribution cover the models in the table.

The discovery reach for a given model is determined by a fitting procedure similar to the one used for the analysis of LEP2 data on Bhabha scattering [2, 3]. A negative log-likelihood function is constructed by combining all simulated data points:

$$-\log \mathcal{L} = \sum_{r=1}^n \left(\frac{[\text{prediction}(\text{SM}, \varepsilon) - \text{measurement}]^2}{2 \cdot \Delta^2} \right)_r \quad (2)$$

where $\text{prediction}(\text{SM}, \varepsilon)$ is the SM expectation for a given measurement (cross section or forward-backward asymmetry) combined with the additional effects of new physics as a function of their characteristic scale, measurement is the corresponding measured (here simulated) quantity and $\Delta = \text{error}[\text{prediction}(\text{SM}, \varepsilon) - \text{measurement}]$. The index r runs over all data points. For contact interactions

$$\varepsilon = \frac{1}{\Lambda^2}. \quad (3)$$

The error on a deviation consists of three parts, which are combined in quadrature: a statistical error, a systematic error (our best guess) and a theoretical uncertainty (expected to be in general quite small, but still important for large accumulated luminosities). One-sided lower limits (i.e. the sensitivity) on the scale (e.g. Λ for contact interactions) at 95% confidence level are derived for the two possible signs of the interference terms. This is done by integrating the log-likelihood functions in the physically allowed range of the parameters describing new physics phenomena, assuming a uniform prior distribution.

2.1 Drell-Yan at the Large Hadron Collider

In the Standard Model the production of lepton pairs in hadron-hadron collisions, the Drell-Yan process [4], is described by s -channel exchange of photons or Z bosons. The parton cross section in the center-of-mass system has the form:

$$\frac{d\sigma}{d\Omega} = \frac{\alpha^2}{4s} [A_0(1 + \cos^2 \theta) + A_1 \cos \theta] \quad (4)$$

where $\sigma = \frac{4\pi\alpha^2}{3s} A_0$, $A_{\text{FB}} = \frac{3}{8} \frac{A_1}{A_0}$ give the total cross section and the forward-backward asymmetry. The terms A_0 and A_1 are fully determined by the electroweak couplings of the initial- and final-state fermions. At the Z peak the Z exchange is dominating and the interference term is vanishing. At higher energies both photon and Z exchange contribute and the large value of the forward-backward asymmetry is due to the interference between the neutral currents.

Fermion-pair production above the Z pole is a rich search field for new phenomena at present and future high energy colliders. The differential cross section is given by

$$\frac{d\sigma}{d\Omega} = |\gamma_s + Z_s + \text{New Physics ?!}|^2 \quad (5)$$

where many proposed types of new physics can lead to observable effects by adding new amplitudes or through their interference with the neutral currents of the SM.

At hadron colliders the parton cross sections are folded with the parton density functions (PDF): $pp \rightarrow l_1 l_2$

$$\frac{d^2\sigma}{dM_{ll}dy} [pp \rightarrow l_1 l_2] \sim \sum_{ij} \left(f_{i/p}(x_1) f_{j/p}(x_2) + (i \leftrightarrow j) \right) \hat{\sigma} \quad (6)$$

$\hat{\sigma}$ - cross section for the partonic subprocess $ij \rightarrow l_1 l_2$

$M_{ll} = \sqrt{\tau s} = \sqrt{\hat{s}}$ - mass, y - rapidity of the lepton pair

$x_1 = \sqrt{\tau} e^y, x_2 = \sqrt{\tau} e^{-y}$ - parton momentum fractions,

$f_{i/p(\bar{p})}(x_i)$ - probability to find a parton i with momentum fraction x_i in the (anti)proton.

$$\sigma_{F\pm B}(y, M) = \left[\int_0^1 \pm \int_{-1}^0 \right] \sigma_{ll} d(\cos \theta^*) \quad (7)$$

$$A_{FB}(y, M) = \frac{\sigma_{F-B}(y, M)}{\sigma_{F+B}(y, M)}. \quad (8)$$

Table 2: x_1 and x_2 for different masses and rapidities.

y	0	2	4
$M = 91.2 \text{ GeV}$			
x_1	0.0065	0.0481	0.3557
x_2	0.0065	0.0009	0.0001
$M = 200 \text{ GeV}$			
x_1	0.0143	0.1056	0.7800
x_2	0.0143	0.0019	0.0003
$M = 1000 \text{ GeV}$			
x_1	0.0714	0.5278	-
x_2	0.0714	0.0097	-

The total cross section and the forward-backward asymmetry are function of observables which are well measured experimentally for e^+e^- and $\mu^+\mu^-$: the invariant mass and the rapidity of the final state lepton-pair. This allows to reconstruct the center-of-mass energy of the initial partons, even if their flavors are unknown. This will be used in the subsequent analysis of contact interactions by performing a scan of the high mass region above 0.5 TeV. For a ($x_1 \geq x_2$) pair of partons we have 4 combinations of *up*- or *down*-type quarks initiating the interaction: $u\bar{u}, \bar{u}u, d\bar{d}, \bar{d}d$. In pp collisions the antiquarks come always from the sea and the quarks can have valence or sea origin. The x -range probed depends on the mass and rapidity of the lepton-pair as shown in Table 2. Going to higher rapidities increases the difference between x_1 and x_2 and hence the probability that the first quark is a valence one. This allows a measurement of the forward-backward asymmetry even for the symmetric initial pp state.

Events are generated with the PYTHIA 6.2 Monte Carlo [5] (with default PDF CTEQ5L) by applying the following cuts for both leptons:

- pseudorapidity $|\eta| < 2.5$
- transverse momentum $p_T > 20 \text{ GeV}$

which cover the barrel and endcaps of a typical LHC detector. The backgrounds for these final states are low and can be suppressed further by isolation cuts. It is interesting to enlarge the acceptance to the very forward region. Experimentally this is very demanding and will not be considered here. Everywhere in this study only acceptance cuts are applied and the experimental efficiency within this region is kept at 100 %. For lower efficiency the luminosity for obtaining the same result has to be rescaled accordingly. The results presented here are an extension of the studies for the LHC SM workshop (see [6,7] and references therein), using much higher statistics and applying a rigorous statistical procedure to determine the sensitivity reach.

Table 3: Sensitivity reach in one experiment for contact interactions (LL model) at 95% CL at LHC.

$pp \rightarrow e^+e^-X, \mu^+\mu^-X$ One Experiment				
Contact Interactions LL Model				
	3 % syst. err.		6 % syst. err.	
Luminosity [fb^{-1}]	Λ^- [TeV]	Λ^+ [TeV]	Λ^- [TeV]	Λ^+ [TeV]
1	22.1	19.0	22.1	19.0
10	31.8	24.3	31.7	24.2
100	56.9	32.0	51.7	31.0

The effects of contact interactions are investigated for the LL model, which is incorporated in PYTHIA. The statistical procedure is as outlined above. In contrast to the linear collider case, where we have developed a semi-analytical program with numeric integrations, here we are using a Monte-Carlo generator. So the task of computing the new physics predictions for a large enough set of values of the scale Λ is much more CPU intensive. We generate 100000 events for each scale value to keep the Monte-Carlo error small and repeat the generation 200 times to cover a wide enough range of scales. For the linear collider studies we use a set with 800 values of the scale for each case, and they are much faster to compute with a semi-analytical program.

The sensitivity reaches from our fits for different luminosities are summarized in Table 3, assuming that we detect electron- and muon-pairs in one LHC experiment. The sensitivity is dominated by the cross section measurement, the contribution of the forward-backward asymmetry is minor due to the large statistical errors and the need to apply rapidity cuts. Clearly ATLAS and CMS can combine their data. The sensitivity ranges from 19.0 to 32.0 TeV for positive and from 22.1 to 56.9 TeV for negative interference. The effects of contact interactions on the Drell-Yan mass spectrum are illustrated in Figure 1. Compared to the sensitivity reach for hadronic final states at a linear collider [8], the positive interference case is similar and the negative interference case more sensitive. But a linear collider can detect also specific flavors, e.g. beauty or charm final states, where the sensitivity is higher. So an indication of something new from LHC can be studied in much greater detail at a FLC. Even at the highest luminosities the statistical errors at LHC are dominant, as evident from the comparison of the cases with total systematic uncertainties

LHC 100 fb⁻¹ One Exp.

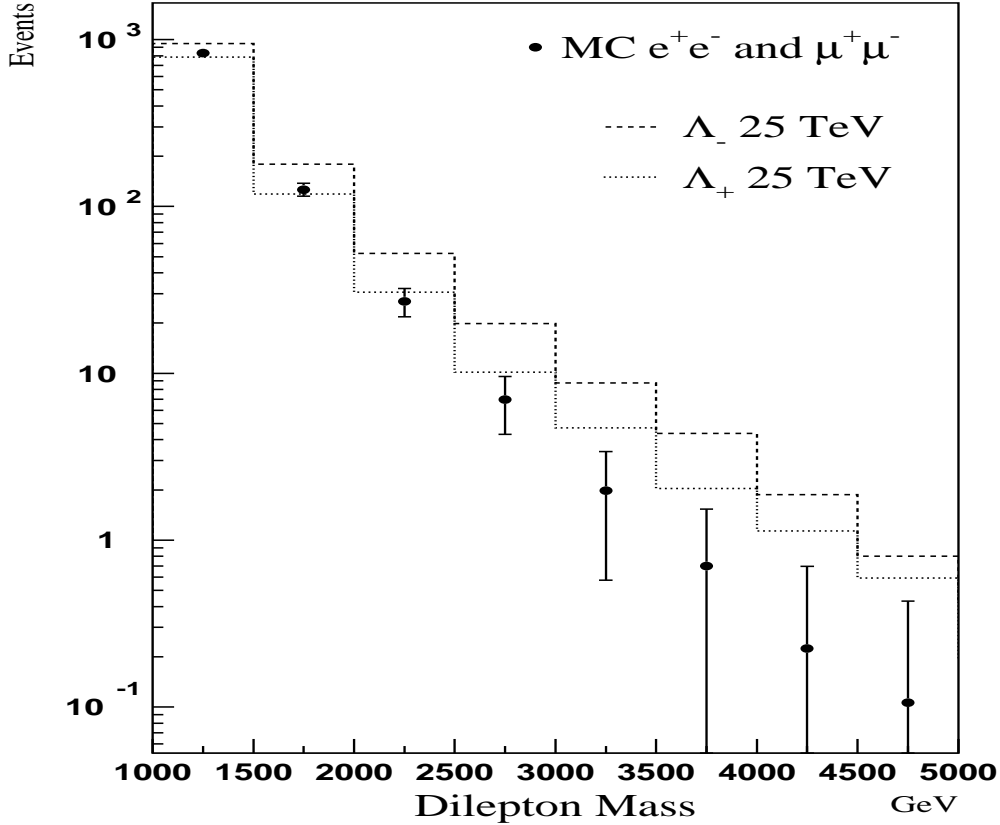


Figure 1: *Effects of contact interactions on the dilepton mass spectrum. Points are simulated events in the SM, and the histograms show the spectrum in the presence of LL contact interactions with different signs of the amplitudes.*

of 3 and 6 %. This is not surprising as the Drell-Yan process is probing directly masses up to $\sim 3\text{--}4$ TeV, where due to the steeply falling cross sections the statistical errors dominate by far.

2.2 e^+e^- at a Linear Collider

The effects of new physics at a linear collider with $\sqrt{s} = 0.5$ TeV are computed with a semi-analytical program in the improved Born approximation, using effective couplings. QED effects in the initial and final states are taken into account. Events without substantial energy loss due to initial state radiation are selected by a cut on the “effective” energy: $\sqrt{s'}/\sqrt{s} > 0.85$. For them the interactions occur close to the nominal machine energy and offer the best sensitivity for manifestations of new physics. We repeat the computation for each case under study (e.g. one of the eight contact interaction models) for a set of 800 values of the relevant scale. The sensitivity to contact interactions is determined by a fit as outlined above.

Two cases are distinguished:

1. “Realistic”: a cross section error is composed of the statistical error and a systematic

Table 4: Sensitivity reach for contact interactions at 95% CL at a linear collider with $\sqrt{s} = 0.5$ TeV and 1000 fb^{-1} .

$e^+e^- \rightarrow e^+e^-$				
Contact Interactions				
Model	"Realistic"		Optimistic	
	Λ^- [TeV]	Λ^+ [TeV]	Λ^- [TeV]	Λ^+ [TeV]
LL	23.2	23.3	43.5	44.9
RR	22.5	22.5	42.1	43.4
VV	43.9	45.2	83.3	89.1
AA	32.5	35.0	71.9	77.1
LR	25.2	24.4	50.7	52.4
RL	25.2	24.4	50.7	52.4
LL+RR	32.0	32.6	59.9	63.0
LR+RL	35.0	35.2	71.0	75.0

error of 0.5 % coming from the experiment, 0.2 % from the luminosity determination and a theoretical uncertainty of 0.5 %. The forward-backward asymmetry error consists of the statistical error and a systematic uncertainty of 0.002 (absolute) for e^+e^- and 0.001 (absolute) for $\mu^+\mu^-$ final states. The main origins of the latter are from charge confusion of the leptons and uncertainties in the acceptance edge determination. Both of these effects are more important for electrons due to the forward peak in the differential cross section and the longer lever arm for measuring the muon momenta. One should stress that the forward-backward asymmetry systematics is lower than what was achieved at LEP, and requires a substantially improved detector.

2. Optimistic: a cross section error is composed just of the statistical error and a 0.2 % contribution from the luminosity determination. The forward-backward asymmetry error consists of the statistical error and a systematic uncertainty which is given by the *minimum* of the systematic uncertainty for the "Realistic" case and the statistical error. The rationale behind is the hope that with increasing statistics one can control the systematic effects better. In practice this turns out to play a role only for e^+e^- . For $\mu^+\mu^-$ the statistical error of the forward-backward asymmetry is always bigger than 0.001.

The optimization of the acceptance range is an important experimental question. The strong forward peak of Bhabha scattering is less sensitive to new physics as the SM amplitudes dominate the interference terms. We have investigated two regions:

- barrel: from 44° to 136° , where the polar angle is with respect to the electron beam line

- barrel + backward endcap: from 44° to 170° , so the region of backward scattering is added.

For contact interactions there is no gain from going outside of the barrel region, even the sensitivity reach is reduced by 1–2 %. As the detector performance is usually highest, and the backgrounds lowest in the central region, this is the optimal measurement area from experimental point of view.

Table 5: Sensitivity reach for contact interactions at 95% CL at a linear collider with $\sqrt{s} = 0.5$ TeV for the VV model with positive interference as a function of the accumulated luminosity.

$e^+e^- \rightarrow e^+e^-$		
VV Model		
	“Realistic”	Optimistic
Luminosity [fb^{-1}]	Λ^+ [TeV]	Λ^+ [TeV]
1	27.3	28.4
10	39.8	49.9
100	44.4	74.8
1000	45.2	89.1

The sensitivity reaches from our fits for the different models are summarized in Table 4. They range from 22.5 to 45.2 TeV in the “Realistic” scenario and are factor of two higher in the Optimistic case, which should be taken as an “ideal” upper sensitivity limit. The estimates for muon pairs in [8] are somewhat higher for 1000 fb^{-1} . They are derived under more optimistic assumptions and use in addition the left-right asymmetry, which is not included in the present study. The limits from Bhabha scattering at LEP are factor of 2.6–2.9 lower [3,9,10].

The sensitivity reach for e.g. the VV model evolves from 27.3 TeV at start-up to 44.4 TeV for 100 fb^{-1} , where it is saturated by the systematic effects as depicted in Table 5.

3 Extra Spatial Dimensions

The development of string theory points to the existence of up to seven additional dimensions, which are compactified at very small distances, initially estimated to be $\sim 10^{-32}$ m, and hence far below the scales probed at high energy colliders. In a radical proposal [11, 12], the hierarchy problem is dealt with by bringing close the electroweak scale $m_{EW} \sim 1$ TeV and the Planck scale $M_{Pl} \sim \frac{1}{\sqrt{G_N}} \sim 10^{15}$ TeV. In this framework the effective four-dimensional M_{Pl} is connected to a new $M_{Pl(4+n)}$ scale in a $(4+n)$ dimensional theory:

$$M_{Pl}^2 \sim M_{Pl(4+n)}^{2+n} R^n \quad (9)$$

where there are n extra compact spatial dimensions of radius $\sim R$, which could be probed at present and future colliders. This can explain the observed weakness of gravity at large distances. At the same time, quantum gravity becomes strong at a scale M of the order of few TeV and could have observable signatures. The attractiveness of this proposal is enhanced by the plethora of expected phenomenological consequences described by just a few parameters.

In the production of fermion- or boson-pairs in e^+e^- or pp collisions this class of models can be manifested through virtual effects due to the exchange of gravitons (Kaluza-Klein excitations). As discussed in [16, 13, 14, 15, 17], the exchange of spin-2 gravitons modifies in a unique way the differential cross sections for fermion pairs, providing clear signatures. These models introduce an effective scale (cut-off), denoted as M_s in [16, 17], as \mathcal{L}_T in [13] and again as M_s in [14]. The first two scales are connected by the relation $M_s = (2/\pi)^{1/4}\Lambda_T$, which gives numerically $\mathcal{L}_T = 1.1195 M_s$. They do not depend on the number of extra dimensions. In the third case the scale exhibits such a dependence; the relation to the other scales is given by $M_s^{HLZ}|_{n=4} = \mathcal{L}_T$ for four extra dimensions.

Table 6: Sensitivity reach for extra dimensions at 95% CL at a linear collider with $\sqrt{s} = 0.5$ TeV for the Hewett scale and positive interference as a function of the accumulated luminosity.

$e^+e^- \rightarrow e^+e^-$		
Hewett Scale		
	“Realistic”	Optimistic
Luminosity [fb^{-1}]	M_s [TeV]	M_s [TeV]
1	2.6	2.6
10	3.1	3.5
100	3.3	4.2
1000	3.3	4.6
$e^+e^- \rightarrow \mu^+\mu^-$		
Hewett Scale		
	“Realistic”	Optimistic
Luminosity [fb^{-1}]	M_s [TeV]	M_s [TeV]
1	1.6	1.6
10	2.1	2.1
100	2.8	2.8
1000	3.5	3.5

We will use the scale M_s of [16] throughout this paper. The cut-off scale is supposed to be of the order of the fundamental gravity scale M in $4+n$ dimensions. The results

are model-dependent, which is usually expressed by the introduction of an additional parameter

$$\varepsilon = \frac{\lambda}{M_s^4}. \quad (10)$$

The value of λ is not known exactly, the usual assumption is $\lambda = \pm 1$ to allow for both constructive and destructive interference effects.

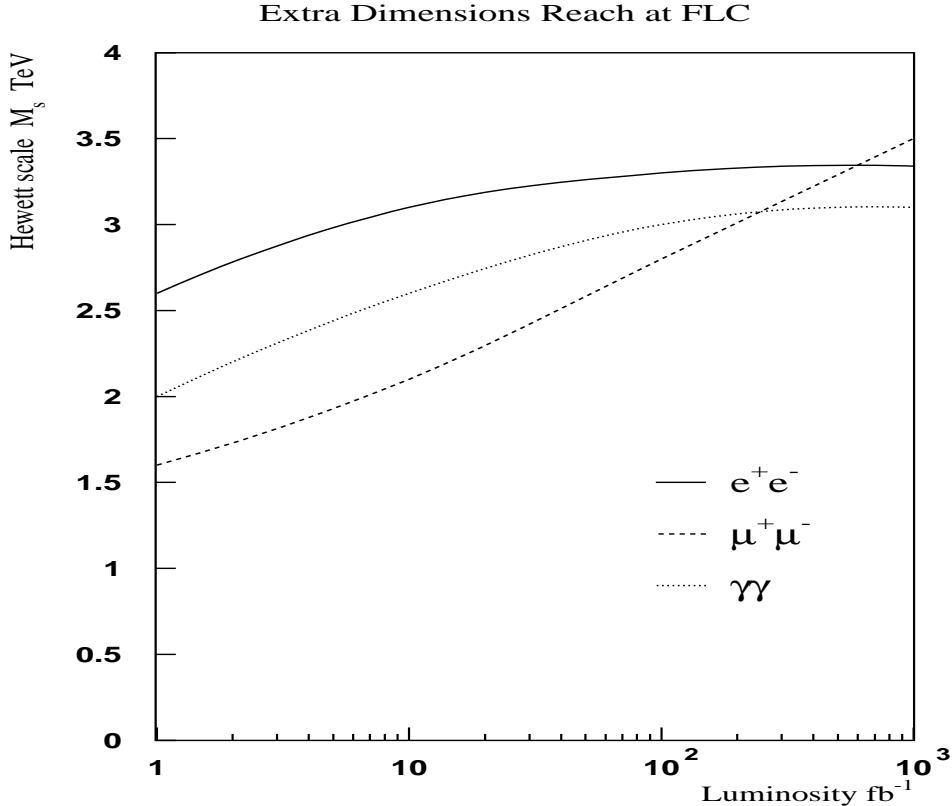


Figure 2: Evolution of the sensitivity reach for extra dimensions at a linear collider with $\sqrt{s} = 0.5$ TeV in different final states with the accumulated luminosity.

3.1 e^+e^- and $\mu^+\mu^-$ at a Linear Collider

The approach is the same as for contact interactions in Bhabha scattering, as discussed earlier. The parameter ε is defined in Equation (10). The virtual graviton effects are computed using the calculations from [16,13,17].

The sensitivity reaches from our fits for electron- and muon-pairs are summarized in Table 6. They evolve from 2.6 (1.6) TeV for electrons (muons) at start-up to 3.3 (2.8) TeV for 100 fb^{-1} . Here the electron channel is saturated by the systematic uncertainties, while the muon channel is taking over for the highest luminosities. In the tables only the numbers for the positive interference case are shown, as the sensitivity reach for negative interference is practically the same. The results are shown in Figure 2 and agree with estimates from [16,17,8].

It is interesting to note the large difference between the “Realistic” and the Optimistic scenarios for the two channels: while the electrons start to saturate above 10 fb^{-1} , the muons do not show any saturation at all. This is explained by the fact that for Bhabhas the sensitivity comes mainly from the cross section measurement, while for muons is it dominated completely by the forward-backward asymmetry, and with our assumptions the statistical error is always bigger than the systematic uncertainties.

We investigate the optimal acceptance region also for extra dimensions. For electrons in the final state the gain in sensitivity is below 1 % from including the backward endcap, so we may as well restrict the measurement to the barrel region. For muons the sensitivity comes from the asymmetry which is best measured at lower angles, so the results in the table are derived under the assumption that both the barrel and the two endcaps are used i.e. from 10° to 170° .

The present limits on the Hewett scale are $\sim 1.3 \text{ TeV}$ from LEP and TEVATRON measurements (see e.g. [18, 19, 20, 21, 10]).

3.2 $\gamma\gamma$ at a Linear Collider

The production of photon pairs in e^+e^- collisions is described by t - and u -channel QED diagrams. The differential cross section has the following simple form

$$\frac{d\sigma}{d\Omega} = |e_t + e_u + \text{New Physics ?!}|^2 \quad (11)$$

$$\left(\frac{d\sigma}{d\Omega}\right)_{QED} = \frac{\alpha^2}{2s} \left[\frac{t}{u} + \frac{u}{t}\right] = \frac{\alpha^2}{s} \cdot \frac{1 + \cos^2\theta}{1 - \cos^2\theta}. \quad (12)$$

Table 7: Sensitivity reach for extra dimensions at 95% CL at a linear collider with $\sqrt{s} = 0.5 \text{ TeV}$ for the Hewett scale, and for the QED cut-off, in the case of positive interference as a function of the accumulated luminosity.

$e^+e^- \rightarrow \gamma\gamma$		
Hewett Scale		
	“Realistic”	Optimistic
Luminosity [fb^{-1}]	M_s [TeV]	M_s [TeV]
1	2.0	2.0
10	2.6	2.6
100	3.0	3.4
1000	3.1	4.1
$\Lambda^{QED} 1000$	1.2	1.6

Deviations from QED typically have the form:

$$\frac{d\sigma}{d\Omega} = \left(\frac{d\sigma}{d\Omega} \right)_{QED} \cdot \left(1 \pm \frac{1}{(\mathbb{L}_{\pm}^{QED})^4} \cdot \frac{s^2}{2} \sin^2 \theta \right) \quad (13)$$

$$\frac{d\sigma}{d\Omega} = \left(\frac{d\sigma}{d\Omega} \right)_{QED} \cdot \left(1 \pm \frac{\lambda}{\pi\alpha(M_s)^4} \cdot \frac{s^2}{2} \sin^2 \theta + \dots \right) \quad (14)$$

The QED cut-off - Equation (13), is the basic form of possible deviations from quantum electrodynamics. Equation (14) is the low scale gravity case [13,22]. If we ignore higher order terms (given by ...), the equations predict the same form of deviations in the differential cross section. In this notation, it is particularly easy to compare the results from different searches by transforming the relevant parameters. The relation between the Hewett scale and the QED cut-off is:

$$M_s = 2.57 \mathbb{L}^{QED}.$$

The sensitivity reach from our fits is summarized in Table 7. The sensitivity evolves from 2 TeV at start-up to 3 TeV for 100 fb⁻¹, where it is saturated by the systematic effects. The LEP limits are ~ 1 TeV [23,18,10]. As for Bhabhas, there is no gain in sensitivity going outside of the barrel region. Here the differential cross section is symmetric, exhibiting both a forward and a backward peak.

Table 8: Sensitivity reach for extra dimensions at 95% CL at a linear collider with $\sqrt{s} = 0.5$ TeV for the Hewett scale and positive interference as a function of the accumulated luminosity.

$e^+e^- \rightarrow e^+e^-, \mu^+\mu^-, \gamma\gamma$		
Hewett Scale		
	“Realistic”	Optimistic
Luminosity	M_s	M_s
[fb ⁻¹]	[TeV]	[TeV]
1	2.6	2.6
10	3.2	3.5
100	3.5	4.3
1000	3.8	4.8

If we combine the results from $\gamma\gamma, e^+e^-$ and $\mu^+\mu^-$, we get the sensitivity shown in Table 8. Scales up to 3.8 TeV can be probed.

Acknowledgments

This work is supported in part by the United States National Science Foundation under grants NSF ITR-0086044 and NSF PHY-0122557.

References

- [1] E. Eichten, K. Lane and M. Peskin, Phys. Rev. Lett. **50** (1983) 811.
- [2] D. Bourilkov, JHEP **9908** (1999) 006 [arXiv:hep-ph/9907380].
- [3] D. Bourilkov, Phys. Rev. D **62** (2000) 076005 [arXiv:hep-ph/0002172].
- [4] S.D. Drell and T-M. Han, Phys. Rev. Lett. **25** (1970) 316.
- [5] T. Sjöstrand *et al.*, Comp. Phys. Commun. **135** (2001) 238.
- [6] S. Haywood *et al.*, arXiv:hep-ph/0003275.
- [7] D. Bourilkov, CMS IN 2000/035, CERN, 2000.
- [8] S. Riemann, LC-TH-2001-007.
- [9] D. Bourilkov, Phys. Rev. D **64** (2001) 071701 [arXiv:hep-ph/0104165].
- [10] D. Abbaneo *et al.*, arXiv:hep-ex/0212036.
- [11] N. Arkani-Hamed, S. Dimopoulos and G. Dvali, Phys. Lett. B **429** (1998) 263.
- [12] I. Antoniadis, N. Arkani-Hamed, S. Dimopoulos and G. Dvali, Phys. Lett. B **436** (1998) 257.
- [13] G. Giudice, R. Rattazi and J. Wells, Nucl. Phys. B **544** (1999) 3.
- [14] T. Han, J.D. Lykken and R-J. Zhang, Phys. Rev. D **59** (1999) 105006.
- [15] S. Nussinov and R. Shrock, Phys. Rev. D **59** (1999) 105002.
- [16] J. Hewett, Phys. Rev. Lett. **82** (1999) 4765.
- [17] T. Rizzo, Phys. Rev. D **59** (1999) 115010.
- [18] D. Bourilkov, arXiv:hep-ex/0103039.
- [19] G. Landsberg, arXiv:hep-ex/0105039.
- [20] J. Hewett and M. Spiropulu, Ann. Rev. Nucl. Part. Sci. **52** (2002) 397 [arXiv:hep-ph/0205106].
- [21] K. Cheung, arXiv:hep-ph/0305003.
- [22] K. Agashe, N.G. Deshpande, Phys. Lett. B **456** (1999) 60.
- [23] S. Mele and E. Sanchez, Phys. Rev. D **61** (2000) 117901.